Journal of Power Sources 180 (2008) 535–538

Contents lists available at ScienceDirect

Journal of Power Sources

journal homepage: www.elsevier.com/locate/jpowsour

Short communication

Comparative studies of reaction rates of NH_3 with MgH_2 and LiH

Tippawan Markmaitree, William Osborn, Leon L. Shaw*

Department of Chemical, Materials and Biomolecular Engineering, University of Connecticut, 97 North Eagleville Road, U-3136 Storrs, CT 06269-3136, USA

ARTICLE INFO

Article history:
Received 7 January 2008
Received in revised form 5 February 2008
Accepted 6 February 2008
Available online 10 March 2008

Keywords:
Hydrogen storage materials
Reaction kinetic
MgH_2
LiH
$LiNH_2$

ABSTRACT

The reaction rate of MgH_2 with NH_3 is studied using a two-layered structure containing a top MgH_2 layer and a bottom $LiNH_2$ layer. Quantification of the effluent gas composition from the two-layered structure indicates substantial NH_3 emission, while the X-ray diffraction analysis reveals little formation of the reaction products between MgH_2 and NH_3. In contrast, the study of the two-layered structure containing a top LiH layer and a bottom $LiNH_2$ layer reveals that the reaction between LiH and NH_3 is much faster than that between MgH_2 and NH_3.

1. Introduction

Hydrogen sorption and desorption behavior and mechanisms of the lithium amide ($LiNH_2$) and lithium hydride (LiH) mixture have been studied extensively for its potential as hydrogen storage materials [1–17]. It is generally agreed that the overall dehydriding reaction of this system can be expressed as [1]

$$LiNH_2 + LiH \rightarrow Li_2NH + H_2. \quad (1)$$

Furthermore, many studies [4,5,11,17] have indicated that Reaction (1) proceeds with two elementary reactions. First, $LiNH_2$ decomposes to produce lithium imide (Li_2NH) and ammonia (NH_3), as shown in Reaction (2).

$$2LiNH_2 \rightarrow Li_2NH + NH_3. \quad (2)$$

Then, LiH reacts with NH_3 to form $LiNH_2$ again and liberate H_2, as shown in Reaction (3).

$$NH_3 + LiH \rightarrow LiNH_2 + H_2. \quad (3)$$

For a mixture of $LiNH_2$ + LiH (with a molar ratio of 1:1), the reaction would continue to repeat the cycle of Reactions (2) and (3) until all $LiNH_2$ and LiH transform to lithium imide (Li_2NH) and H_2 completely. The reaction rate of LiH with NH_3 has been shown to be very fast, in the order of microsecond [4]. This feature has been proven to be critical in avoiding NH_3 emission from the $LiNH_2$ + LiH mixture [11,17].

In spite of the high storage capacity and fast reaction rate between LiH and NH_3, the lithium imide/amide/hydride system still requires relatively high operating temperatures (~280 °C) to obtain 1 atm of hydrogen sorption and desorption pressure [1–17]. In order to increase the equilibrium pressure and lower the sorption and desorption temperatures, many studies have focused on destabilization of lithium amide through partial substitution of lithium by magnesium [7,8,12,18–36]. This approach has indeed resulted in encouraging results. For example, the ($2LiNH_2 + MgH_2$) system has been demonstrated to absorb and desorb 5.2 wt.% of hydrogen with a hydrogen pressure of 30 atm at 200 °C [19,20], showing a much higher hydrogen pressure than the lithium imide/amide/hydride system at this temperature. However, recent works [35,36] indicate that LiH-containing systems have faster hydriding and dehydriding reaction kinetics than MgH_2-containing systems. Furthermore, it is found that the $MgH_2/LiNH_2$ system exhibits NH_3 emission, whereas the $LiH/LiNH_2$ system does not, or its NH_3 emission, if any, is below the detection limit of the mass spectrometer [36]. It is suggested that the slow kinetics of MgH_2-containing systems is due to the sluggish reaction between MgH_2 and NH_3 [35,36]. This proposal is consistent with the observation that the reaction kinetic between LiH and NH_3 during ball milling at room temperature is faster than that between MgH_2 and NH_3 under the same ball milling condition [35,37]. In this study, we have used a two-layered powder structure described by Hu and Ruckenstein [4] to compare the reaction rates of NH_3 with MgH_2 and with LiH at high temperatures up to 450 °C. Such a study is necessary because hydriding and dehydriding reactions of LiH- and MgH_2-containing systems are all currently carried out at temperatures above ambient [1–36].

* Corresponding author. Tel.: +1 860 486 2592; fax: +1 860 486 4745.
E-mail address: leon.shaw@uconn.edu (L.L. Shaw).

0378-7753/$ – see front matter © 2008 Elsevier B.V. All rights reserved.
doi:10.1016/j.jpowsour.2008.02.037

2. Experimental

In order to compare reaction rates of NH_3 with MgH_2 and with LiH, an experimental setup of a two-layered powder structure described in Ref. [4] were utilized in this study. Specifically, LiH or MgH_2 powder of a known quantity was placed on top of a layer of $LiNH_2$ powder in an alumina-microbalance crucible which was subsequently loaded into a thermogravimetric (TG) analyzer (TA instrument, TGA Q500). The weight ratios of LiH to $LiNH_2$ and MgH_2 to $LiNH_2$ in the two-layered setup depend on the quantitative relationship to be evaluated in each experiment. Table 1 summarizes all the ratios that were investigated in this study. These experimental setups allowed us to evaluate effects of the molar ratio, surface area ratio, and volume ratio of the hydrides to $LiNH_2$. Note that the two-layered powder structure was used in this study because the specific surface area of the individual component involved could be controlled precisely, which would not be the case if the ball-milled powder mixture were used for investigation. All the powder handling was performed in a glovebox before being transferred to the TG analyzer. The transfer resulted in a short exposure of the sample to air (less than 30 s) and the loaded TG analyzer was flushed immediately with Ar of 99.999% purity for 90 min before heating. This Ar flushing at room temperature for 90 min is necessary to minimize oxidation of hydrides in the subsequent heating process.

$LiNH_2$ with 95% purity was purchased from Fisher Scientific, while LiH with 95% purity and MgH_2 with 98% purity were purchased from Alfa Aesar. All the as-purchased LiH, $LiNH_2$ and MgH_2 powders were subjected to ball milling for 45 min using a modified Szegvari attritor in order to produce powders with the desired specific surface areas which can facilitate the direct comparison of the reaction rates of NH_3 with MgH_2 and LiH. The ball-milled powders were then used to set up the two-layered structure, as described above, which was subsequently heated with a heating rate of 5 °C min^{-1} up to 450 °C using the TG analyzer. The flow rate of argon of 99.999% purity was maintained at 60 ml min^{-1} in the entire heating process. The outlet gas from the TG analyzer was constantly monitored using a quadrupole residual gas analyzer (RGA) equipped with a mass spectrometer (Model ppt-c300-F2Y). The gases monitored included H_2, NH_3, N_2, O_2, and H_2O. The RGA unit was calibrated using two gas-mixture calibrations, with one containing 21.71 vol.% H_2 and 78.29 vol.% Ar and the other 301 ppm N_2, 1210 ppm O_2, 1990 ppm NH_3, and Ar balance.

The specific surface area (SSA) of each powder after high-energy ball milling was determined through nitrogen adsorption at 77 K based on the Brunauer–Emmett–Teller (BET) method [38] using a gas sorption analyzer (NOVA 1000). The measured SSA was used to calculate the surface area ratio of the hydride to $LiNH_2$ in the two-layered structure. Similarly, the volume of each component in the two-layered structure was computed by dividing the measured sample weight by the density of the component involved. The molar ratio of the hydride to $LiNH_2$ in the two-layered structure was determined in a similar manner by involving the measured and molar weights of each component. The molar ratios, surface area ratios, and volume ratios of all the hydride to $LiNH_2$ samples are summarized in Table 1.

In order to identify the solid products formed from the two-layered structure, the samples before and after different heating schedules at different locations within the two-layered structure were analyzed using X-ray diffraction (XRD). The operation conditions for the XRD data collection were Cu Kα radiation, 40 kV, 40 mA, 0.03° min^{-1}, and 0.02°/step using a Bruker D8 Avance diffractometer. To quantify the change in the concentrations of the reactants and products, all the samples were mixed with 10 wt.% coarse-grained Si powder as an internal standard before XRD analysis. To prevent oxidation during XRD data collection, the sample was sealed in a capillary quartz tube and the loading of the sample to the tube was performed in a glove-box filled with argon of 99.999% purity. The capillary quartz tube had a wall thickness of 0.01 mm and thus was transparent to the X-ray.

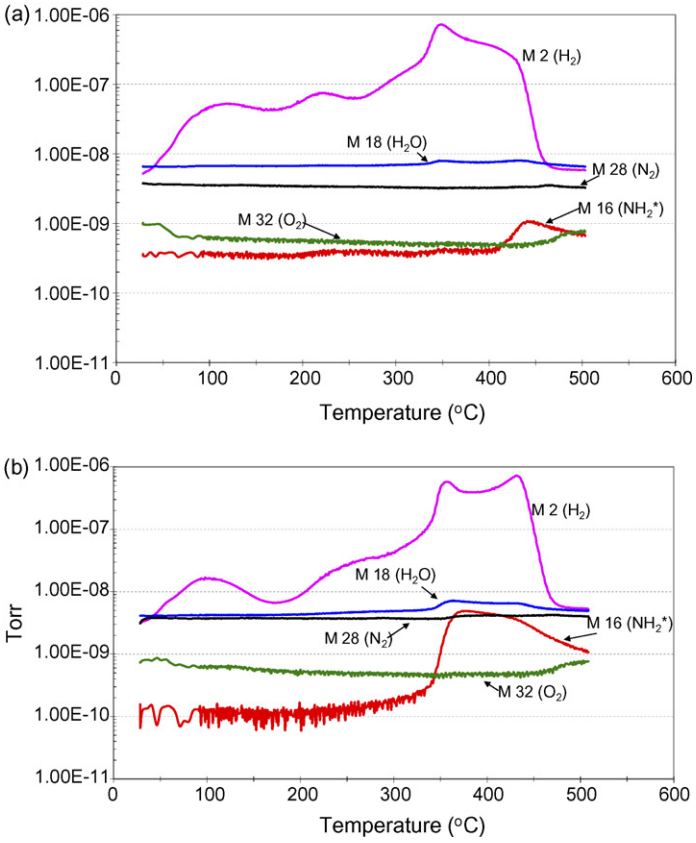

Fig. 1. The composition profile of the effluent gas from (a) the two-layered $LiNH_2$ + LiH system (Sample 1 in Table 1) and (b) the two-layered $LiNH_2$ + MgH_2 system (Sample 2 in Table 1) as a function of temperature. The heating rate is 5 °C min^{-1} with an argon flowing rate of 60 ml min^{-1} in in the entire heating process.

3. Results and discussion

Fig. 1 shows the composition profile of the effluent gas from Sample 1 ($LiNH_2$ + LiH system) and Sample 2 ($LiNH_2$ + MgH_2 system) as a function of temperature during heating. Several phenomena are noted. First, H_2 is clearly the major component of the effluent gas for both ($LiNH_2$ + MgH_2) and ($LiNH_2$ + LiH) systems. Second, N_2, O_2 and H_2O concentrations change little in the entire heating process. Third, the NH_3 concentration, quantified using the intensity of NH_2^+ species with the mass-to-charge ratio of 16 (called M16 hereafter), I_{M16}, is much higher for the ($LiNH_2$ + MgH_2) system than the ($LiNH_2$ + LiH) system. The intensity of NH_3^+ species was not used to quantify NH_3 because of the presence of OH^+ species the intensity of which is 21.2% of the H_2O^+ intensity [17]. Fourth, the onset temperature for hydrogen release appears to be very low (starting almost at the onset of heating). This is likely due to the reaction between the hydride and a trace amount of oxygen in the TG chamber, which results in the first hydrogen peak at about 90 °C. However, all the other hydrogen peaks at higher temperatures are related to the reactions between hydrides and NH_3 because they coincide with the increase of the NH_3 concentration in the effluent gas. Emission of the NH_3 from the decomposition of $LiNH_2$ and the H_2 from the reaction between the hydride and NH_3 forms a blanket to prevent oxidation of the hydride at higher temperatures. Finally, it is noted that a substantial amount of H_2 is released at or above 400 °C, which is almost 200 °C higher than the previous

Table 1
The molar ratio, surface area ratio, and volume ratio of the hydride to $LiNH_2$ in the two-layered structures and the NH_3 concentrations in the effluent gases from these two-layered structures

Sample ID	System	Molar ratio hydride/$LiNH_2$	Surface area ratio hydride/$LiNH_2$	Volume ratio hydride/$LiNH_2$	NH_3 conc. (ppm)
Sample 1	$LiNH_2$ + LiH	1.144	2.276	0.570	387
Sample 2	$LiNH_2$ + MgH_2	0.975	4.184	0.929	2670
Sample 3	$LiNH_2$ + LiH	1.927	3.833	0.959	27
Sample 4	$LiNH_2$ + MgH_2	0.930	3.993	0.886	3132

reported data [17,35,36]. The discrepancy is attributed to the current two-layered structure in contrast to the ball-milled mixture in the previous reports [17,35,36].

In order to provide quantitative comparisons in NH_3 emission, the NH_3 concentrations determined from the effluent gas profiles were analyzed based on the molar ratio, surface area ratio, and volume ratio of the hydride to $LiNH_2$, as summarized in Table 1. As shown in Reaction (2), the $LiNH_2$ in the bottom of the two-layered structure will decomposes to Li_2NH and NH_3 during heating. The newly formed NH_3 gas will then enter the top hydride layer (either LiH or MgH_2) and react with the hydride. If all NH_3 is consumed in the reaction, there will be no NH_3 in the effluent gas. Otherwise, the effluent gas will contain NH_3. For a complete reaction, 1 mol of $LiNH_2$ will need 1 mol of LiH to capture all NH_3 to form H_2, as defined by Reaction (1). In contrast, for the ($LiNH_2$ + MgH_2) system, 1 mol of $LiNH_2$ will only need half a mole of MgH_2 to capture all NH_3, as shown in Reaction (4) [19,20].

$$LiNH_2 + (1/2)MgH_2 \rightarrow (1/2)Li_2MgN_2H_2 + H_2. \quad (4)$$

Thus, a comparison between Samples 1 and 2 (Table 1) indicates that LiH is much more effective in reacting with NH_3 than MgH_2 on the molar ratio basis. As indicated by Reactions (1) and (4), if reaction rates between NH_3 and hydrides are very fast, hydride-to-amide molar ratios of 1:1 and 0.5:1 would be sufficient to capture all NH_3 from $LiNH_2$ + LiH and $LiNH_2$ + MgH_2 systems, respectively. However, Sample 2 with a hydride-to-amide ratio 95% higher than the required 0.5:1 molar ratio still exhibits a high NH_3 concentration (i.e., 2670 ppm) in the effluent gas. In contrast, Sample 1 with only 14% higher than the required 1:1 molar ratio manifests a very low NH_3 concentration (387 ppm), which is only 14.5% of the NH_3 concentraion exhibited by Sample 2. Therefore, it can be concluded that the reaction between NH_3 and MgH_2 is slower than that between NH_3 and LiH when the hydride and $LiNH_2$ in the two-layered structure are loaded with the molar ratios as defined by the mass balance of Reactions (1) and (4). Moreover, the reaction between NH_3 and MgH_2 is still slower than that between NH_3 and LiH even when the hydride and $LiNH_2$ in both systems are loaded in a 1:1 molar ratio.

A comparison between Samples 3 and 4 indicates that when LiH and MgH_2 powders have the similar surface area, the NH_3 concentration in the effluent gas of the ($LiNH_2$ + MgH_2) system will be more than 100 times that of the ($LiNH_2$ + LiH) system. Thus, the reaction rate of NH_3 with LiH per LiH surface area is 100 times faster than that of NH_3 with MgH_2 per MgH_2 surface area. A comparison between Samples 3 and 4 also reveals that the reaction volume per unit time for LiH is about 100 times faster than that for MgH_2, because the NH_3 concentration in the effluent gas of the ($LiNH_2$ + MgH_2) system is about 100 times that of the ($LiNH_2$ + LiH) system when LiH and MgH_2 powders have the similar volume. Such a conclusion can also be obtained by comparing Samples 2 and 3. In short, the present study unambiguously establishes that the reaction rate of NH_3 with LiH per LiH surface area, the reaction volume of LiH per unit time, and the number of moles of the reacted LiH per unit time are all higher than the corresponding values for MgH_2 reacting with NH_3.

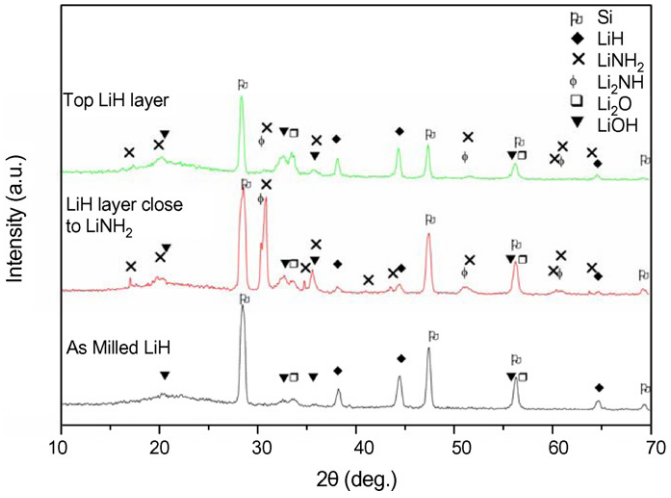

Fig. 2. XRD patterns of the LiH layers before and after heating at different locations within the LiH/$LiNH_2$ two-layered structure. The top LiH layer refers to the layer on top of the LiH layer close to the bottom $LiNH_2$ layer. The two-layered structure was heated to 300 °C at 5 °C min^{-1} in the TG analyzer followed by rapid cooling before the XRD analysis.

Fig. 2 shows XRD patterns of the ($LiNH_2$ + LiH) system before and after heating at different locations within the two-layered structure. Note that the as-milled LiH before heating contains a small amount of Li_2O and LiOH which are mainly from the as-purchased LiH powder. After heating at 5 °C min^{-1} to 300 °C in the TG analyzer followed by rapid cooling, the LiH layer close to the $LiNH_2$ layer in the two-layered structure shows the presence of a large amount of $LiNH_2$ with small amounts of the remaining LiH and newly formed Li_2NH. In contrast, the top LiH layer far away from the $LiNH_2$ layer exhibits the formation of only small amounts of $LiNH_2$ and Li_2NH. Using the Si internal standard, the relative amounts of the remaining LiH and newly formed $LiNH_2$ in the LiH layer at different locations have been quantified and summaried in Table 2. It is clear from Table 2 that the degree of the reaction of the top LiH layer with NH_3 is small (i.e., only about 7% LiH has reacted with NH_3 under the experimental condition empolyed). However, the reaction of the LiH layer close to the $LiNH_2$ layer with NH_3 is quite extensive with 82% LiH having reacted with NH_3. As indicated by Reaction (3), the reaction products between LiH and NH_3 are $LiNH_2$ and H_2. Thus, it is expected that the LiH layer close to the $LiNH_2$ layer would contain a large amount of $LiNH_2$ after reaction. This is indeed the case, as revealed in Table 2. It is also noted that a small amount of Li_2NH is present in the LiH layer after reaction. This Li_2NH comes from the decomposition of the newly formed $LiNH_2$, as indicated by Reaction (2). Finally, the concentration of Li_2O in the top LiH layer

Table 2
The degree of the reaction between LiH and NH_3 as quantified by the change in the ratios of LiH (2 0 0) and $LiNH_2$ (1 1 2) intensities to Si (1 1 1) intensity

Intensity ratio	As-milled LiH	Top LiH layer	LiH layer close to $LiNH_2$
I_{LiH}/I_{Si}	0.357	0.332	0.064
I_{LiNH2}/I_{Si}	0.0	0.005	1.136

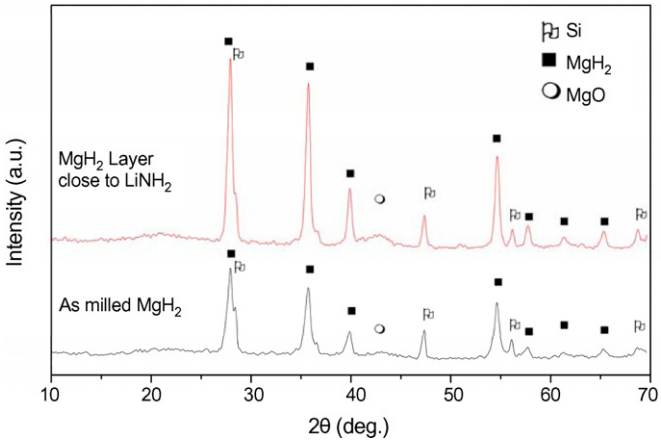

Fig. 3. XRD patterns of the MgH_2 layer before and after heating within the $MgH_2/LiNH_2$ two-layered structure. The two-layered structure was heated to 360 °C at 5 °C min^{-1} in the TG analyzer followed by rapid cooling before the XRD analysis.

is clearly higher than that of the ball-milled counterpart, indicating some oxidation during the TG analysis as discussed previously.

Fig. 3 shows XRD patterns of the MgH_2 layer before and after heating within the two-layered structure. The presence of MgO is attributed to the impurity in the as-purchased MgH_2 powder as well as slight oxidation during ball millnig. After heating at 5 °C min^{-1} to 360 °C in the TG analyzer followed by rapid cooling, the MgH_2 layer close to the $LiNH_2$ layer in the two-layered structure shows no formation of new phases (based on the XRD data only). However, it has been established that the reaction between MgH_2 and NH_3 results in the formation of $Mg(NH_2)_2$ and H_2, as shown below [30,36,37].

$$2NH_3 + MgH_2 \rightarrow Mg(NH_2)_2 + 2H_2. \quad (5)$$

The $Mg(NH_2)_2$ from Reaction (5) can further decompose to form MgNH and NH_3, as shown in Reaction (6) [36]:

$$Mg(NH_2)_2 \rightarrow (1/2)MgNH + (1/2)NH_3. \quad (6)$$

The presence of H_2 in the effluent gas (Fig. 1) and the absence of $Mg(NH_2)_2$ and MgNH in the MgH_2 layer after reaction (Fig. 3) suggest that the reaction between MgH_2 and NH_3 has taken place during heating; however, the reaction rate is slow, and thus the quantities of the $Mg(NH_2)_2$ and MgNH formed from Reactions (5) and (6) are too small to be detected by the XRD analysis. This result is in excellent agreement with the effluent gas analysis (Fig. 1 and Table 1), showing that the reaction between MgH_2 and NH_3 is much slower than that between LiH and NH_3. In order to confirm this conclusion, XRD analysis was also performed for the $MgH_2/LiNH_2$ two-layered structure with a heating rate of 10 °C min^{-1}. The result obtained was similar to that shown in Fig. 3, i.e., no noticeable new phase peaks were found in the MgH_2 layer while there was H_2 and NH_3 emission in the effluent gas.

4. Concluding remarks

The present set of experiments unambiguously establishes that the reaction between MgH_2 and NH_3 is very slow. It is slower than the reaction between LiH and NH_3 on the basis of per hydride surface area, per the reaction volume of the hydride, and per the number of moles of the hydride. Therefore, to minimize the problem of NH_3 emission from $LiNH_2$-containing systems, the use of MgH_2 should be avoided, while LiH should be utilized.

Acknowledgements

This work was supported under the U.S. Department of Energy (DOE) Contract No. DE-FC36-05GO15008. The vision and support of Drs. Carole Read and Ned Stetson, DOE Technology Managers, are greatly appreciated.

References

[1] P. Chen, Z. Xiong, J.Z. Luo, J.Y. Lin, K.L. Tan, Nature 420 (2002) 302–304.
[2] P. Chen, Z. Xiong, J.Z. Luo, J.Y. Lin, K.L. Tan, J. Phys. Chem. B 107 (2003) 10967–10970.
[3] Y.H. Hu, E. Ruckenstein, Ind. Eng. Chem. Res. 42 (2003) 5135–5139.
[4] Y.H. Hu, E. Ruckenstein, J. Phys. Chem. A 107 (2003) 9737–9739.
[5] T. Ichikawa, N. Hanada, S. Isobe, H. Leng, H. Fujii, J. Phys. Chem. B 108 (2004) 7887–7892.
[6] T. Ichikawa, S. Isobe, N. Hanada, H. Fujii, J. Alloys Compd. 365 (2004) 271–276.
[7] S. Orimo, Y. Nakamori, G. Kitahara, K. Miwa, N. Ohba, T. Noritake, S. Towata, Appl. Phys. A 79 (2004) 1765–1767.
[8] T. Ichikawa, N. Hanada, S. Isobe, H. Leng, H. Fujii, Mater. Trans. 46 (2005) 1–14.
[9] Y. Kojima, Y. Kawai, J. Alloys Compd. 395 (2005) 236–239.
[10] Y.H. Hu, E. Ruckenstein, Ind. Eng. Chem. Res. 43 (2004) 2464–2467.
[11] J.H. Yao, C. Shang, K.F. Aguey-Zinsou, Z.X. Guo, J. Alloys Compd. 432 (2007) 277–282.
[12] H.Y. Leng, T. Ichikawa, S. Isobe, S. Hino, N. Hanada, H. Fujii, J. Alloys Compd. 404–406 (2005) 443–447.
[13] G.P. Meisner, F.E. Pinkerton, M.S. Meyer, M.P. Balogh, M.D. Kundrat, J. Alloys Compd. 404–406 (2005) 24–26.
[14] S. Isobe, T. Ichikawa, N. Hanada, H.Y. Leng, M. Fichtner, O. Fuhr, H. Fujii, J. Alloys Compd. 404–406 (2005) 439–442.
[15] T. Ichikawa, N. Hanada, S. Isobe, H.Y. Leng, H. Fujii, J. Alloys Compd. 404–406 (2005) 435–438.
[16] T. Markmaitree, R. Ren, L. Shaw, J. Phys. Chem. B 110 (2006) 20710–20718.
[17] L. Shaw, R. Ren, T. Markmaitree, W. Osborn, J. Alloys Compd. 448 (2007) 263–271.
[18] W. Luo, J. Alloys Compd. 381 (2004) 284–287.
[19] W. Luo, E. Ronnebro, J. Alloys Compd. 404–406 (2005) 392–395.
[20] W. Luo, S. Sickafoose, J. Alloys Compd. 407 (2006) 274–281.
[21] H.Y. Leng, T. Ichikawa, H. Fujii, J. Phys. Chem. B 110 (2006) 12964–12968.
[22] Y. Chen, C.-Z. Wu, P. Wang, H.-M. Cheng, Int. J. Hydrogen Energy 31 (2006) 1236–1240.
[23] Z. Xiong, G. Wu, J. Hu, P. Chen, Adv. Mater. 16 (2004) 1522–1525.
[24] Z. Xiong, J. Hu, G. Wu, P. Chen, W. Luo, K. Gross, J. Wang, J. Alloys Compd. 398 (2005) 235–239.
[25] Z. Xiong, G. Wu, J. Hu, P. Chen, W. Luo, J. Wang, J. Alloys Compd. 417 (2006) 190–194.
[26] Y. Nakamori, S. Orimo, J. Alloys Compd. 370 (2004) 271–275.
[27] H.Y. Leng, T. Ichikawa, S. Hino, N. Hanada, S. Isobe, H. Fujii, J. Phys. Chem. B 108 (2004) 8763–8765.
[28] H.Y. Leng, T. Ichikawa, S. Hino, T. Nakagawa, H. Fujii, J. Phys. Chem. B 109 (2005) 10744–10748.
[29] Y. Nakamori, G. Kitahara, K. Miwa, N. Ohba, T. Noritake, S. Towata, S. Orimo, J. Alloys Compd. 404–406 (2005) 396–398.
[30] Y. Nakamori, G. Kitahara, S. Orimo, J. Power Sources 138 (2004) 309–312.
[31] Y. Nakamori, G. Kitahara, K. Miwa, S. Towata, S. Orimo, Appl. Phys. A 80 (2004) 1–3.
[32] M. Aoki, T. Noritake, G. Kitahara, Y. Nakamori, S. Towata, S. Orimo, J. Alloys Compd. 428 (2007) 307–311.
[33] J. Hu, Z. Xiong, G. Wu, P. Chen, K. Murata, K. Sakata, J. Power Sources 159 (2006) 116–119.
[34] J. Hu, G. Wu, Y. Liu, Z. Xiong, P. Chen, K. Murata, K. Sakata, G. Wolf, J. Phys. Chem. B 110 (2006) 14688–14692.
[35] R. Janot, J.-B. Eymery, J.-M. Tarascon, J. Power Sources 164 (2007) 496–502.
[36] T. Markmaitree, W. Osborn, L. Shaw, Int. J. Hydrogen Energy, in press, doi:10.1016/j.ijhydene.2007.10.052.
[37] H.Y. Leng, T. Ichikawa, S. Hino, N. Hanada, S. Isobe, H. Fujii, J. Power Sources 156 (2006) 166–170.
[38] S. Brunauer, P.H. Emmett, E. Teller, J. Am. Chem. Soc. 60 (1938) 309–319.